A BROADBAND SPECTROMETER FOR DECIMETRIC AND MICROWAVE RADIO BURSTS: FIRST RESULTS

A. O. BENZ, M. GÜDEL, H. ISLIKER, S. MISZKOWICZ, and W. STEHLING

Institute of Astronomy, ETH Zürich, Switzerland

(Received 3 August, 1990; in revised form 12 November, 1990)

Abstract. A new spectrometer has been put into operation that registers solar flare radio emission in the 0.1 to 3 GHz band. It is a frequency-agile system which can be fully programmed to measure both senses of circular polarization at any frequency within that range at selectable bandwidth. The time resolution has to be compromized with the number of frequency channels and can be in the range of 0.5 ms to 250 ms for 1 to 500 channels. First results mainly from the 1–3 GHz band are presented, a spectral region that has never been observed with high-resolution spectrometers. Most noteworthy are the frequent appearances of myriads of narrowband, fast-drifting bursts (microwave type III), diffuse patches of continuum emission, and broad clusters of millisecond spikes sometimes extending from 0.3 to 3 GHz.

1. Introduction

The main energy of solar flares is generally believed to be released in a plasma with an electron density between 10^9 and 10^{12} cm^{-3} (e.g., Antonucci, Rosner, and Tsinganos, 1986; Widing and Doyle, 1990). If the processes involved excite plasma waves or maser emission at a cyclotron harmonic above the plasma frequency, the observable radio emission (if not absorbed) should be in the range roughly between 0.3 and 8 GHz. The 0.3–1.0 GHz band has first been spectrally investigated by Young *et al.* (1961). The 1–3 GHz range is more difficult to observe, since the background of the quiet and slowly varying component becomes appreciable. Thus, it is not surprising that low-resolution spectra obtained by film recording spectrographs in Culgoora and Fort Davis have not shown much detail.

The Radio Astronomy Group of the Institute of Astronomy at the Swiss Federal Institute of Technology (ETH) in Zürich has been engaged in spectral investigation of solar radio bursts since 1972. A first spectrograph, 'Daedalus' (Tarnstrom, 1973) has recorded radio events in the 0.1–1.0 GHz range for more than one cycle. A major result from this effort was the separation of the decimetric bursts intrinsic to the energy release phase of the flare (as characterized by enhanced hard X-ray emission) from the mostly post-flare decimetric type IV outbursts. An overview and a first classification of the extended data set on the impulsive phase has been published by Wiehl, Benz, and Aschwanden (1985). Much higher resolution has become possible with the digital registration technique of the 'Ikarus' spectrometer (Perrenoud, 1982). A catalogue compiled from its data on the impulsive phase has been published by Güdel and Benz (1988). It shows that the impulsive phase bursts in the 0.3–1.0 GHz range can be summarized into type III bursts, pulsations, millisecond spikes, and patches.

Solar Physics **133:** 385–393, 1991.

During the past solar minimum the 'Ikarus' spectrometer has been dismantled and completely rebuilt using some of the old parts. The new instrument, 'Phoenix', operates in a widely extended range with higher frequency stability and new operational possibilities. It is described in Section 2. The new spectrometer has first been used in the 6–8 GHz band in cooperation with the Institute of Applied Physics of the University of Berne. Results of this set-up will be given in a separate article by Bruggmann *et al.* (1990). In Section 3 we present first observations taken since June 1989 in the present spectral range of this instrument from 0.1 to 3 GHz.

2. Instrument

The radio spectrometers of ETH operate by computer control at Bleien, about 50 km west of Zürich. The 'Phoenix' system is fed by a parabolic dish of 7 m diameter with a crossed log-periodic feed in the primary focus covering 0.1 to 4 GHz with a gain of about 7 db. The antenna is presently pointed every 10 s using an 11-bit angle decoder. A continuous guiding system is in preparation.

The thermally-controlled front end close to the focus contains two 90°-hybrids for the ranges above and below 1 GHz to convert the linearly observed polarization into circular polarization, a preamplifier with a noise figure < 4.6 dB, and several PIN-diodes and mechanical switches controlled by the receiver. For standard calibration the feed input can be switched automatically to a noise source with ENR of 35 dB or 25 dB, or to a 50 Ohm resistor. The receiver noise temperature is about 1200 K and only slightly depends on frequency.

In the receiver the signal is first amplified and then up-converted by a 1000 channel direct synthesizer with frequency range from 11.2 to 12.2 GHz, switching speed of 0.45μ (10 to 90%) and an accuracy of 5 ppm. Four 60 MHz bandpass filters with center frequencies of 8.17, 9.17, 10.17, and 11.17 GHz, respectively, are used to suppress image frequencies in the four GHz bands. One of four corresponding quartz-stabilized oscillators at 8.1, 9.1, 10.1, and 11.1 GHz is then selected to mix the signal down to the second intermediate frequency at 70 MHz, where it is further amplified and reduced to 1, 3, or 10 MHz bandwidth. After logarithmic detection in a dynamic range of 80 dB two analog sampling integrators prepare the uncalibrated Stokes parameters I (left plus right circular polarization) and V (left minus right circular polarization) for A/D conversion with 8 bit resolution. Every part in the receiver is controlled by a microstep sequencer (random TTL logic) which is locked to the Swiss normal time standard and supervised by computer.

The measurement duty cycle of 500 μs is subdivided into four main integrating phases of 106 μs each and several switching times used to select frequency, bandwidth, signal source in the front-end, and A/D conversion. In the first and fourth integration interval left circular polarization is observed, in the second and third right circular polarization. Parallel to A/D conversion the receiver is tuned to a new frequency to be observed with selectable bandwidth which is supplied by the system computer from a user-defined list. The result is a scan in frequency which can contain from 1 to 500 observing channels.

Since 2000 such positions are measured per second, the resulting time resolution at one frequency is between 0.5 and 250 ms.

In the regular observing mode the system computer integrates a background scan and records the data on tape only if the flux increases by a certain amount (usually set at about the 5σ level) above the background in a number of channels and for a length of time both to be specified by the user. Signals with extremely steep rise time are interpreted as interference and consequently rejected. In addition to the regular observing mode Dicke-switching to the noise source can be programmed at the cost of polarization measurements, or the data can be digitally integrated on-line by the system computer to save magnetic tape.

The timing of the spectrometer is controlled by a system clock that gets its time information by the public long wavelength signal of Prangin (atomic clock). Thus the relative timing is accurate to less than a microsecond, whereas the absolute time is uncertain to within a few milliseconds due to internal delays.

3. Calibration

Calibration of spectrometers as wide-banded as 'Phoenix' is crucial. Each of the wideband components has its own frequency characteristic. Not only are the dipoles of the feed at different distances from the focus, the receiver gain and noise temperature show considerable variations with frequency. The basic ideas for the calibration of the 'Phoenix' system are similar to the previous 'Ikarus' spectrometer (Perrenoud, 1982). They occur in three steps: (1) The receiver is calibrated against the reference noise source at least once per day. The method includes integrated measurements of the noise source, its attenuated signal, and of a 50 Ohm resistor at 312 K at each frequency. The system computer automatically switches the front end into the appropriate position and steps through the spectrum. From these data are extracted among others: (i) the relation between digital readings at the A/D converter and antenna temperature, and (ii) the receiver noise temperature. (2) In addition to this daily calibration the 50 Ohm resistor can be measured as on-line calibrator in one channel per frequency scan (i.e., normally every 0.1 s). (3) Antenna, feed, and losses up to the first switch are calibrated with the quiet Sun. Other radio sources (e.g., Cas A) have also been used but found less suitable, because their weaker signal yields larger calibration errors. The procedure is time consuming and is carried through once or twice per year. Its goal is to link the flux density of a known point source (the Sun) to the noise source in the front end. The Sun and the background are measured with each linearly polarized feed. These measurements are transformed into degrees Kelvin using the receiver calibration and then give the flux of the Sun as an excess antenna temperature (cf. Figure 1). The small-scale variations with frequency are not noise. They have been found to vary within less than a few percent over weeks. Provided that the Sun is quiet, it is unpolarized to within less than 1%, and using single-frequency observations from other observatories we then find the relations between excess antenna temperature and physical flux units (in erg s^{-1} Hz^{-1} cm^{-2}) and circular polarization.

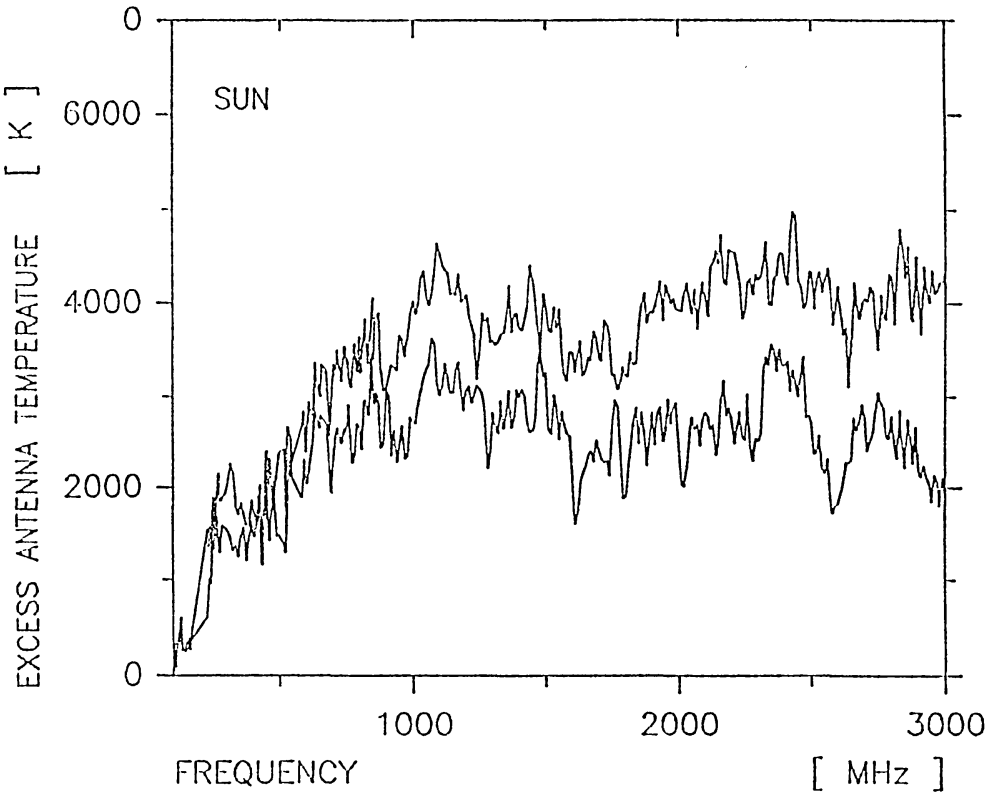

Fig. 1. Excess antenna temperature of the Sun for the two linear, log-periodic feeds vs frequency.

Data calibration is carried out off-line by computer. The daily receiver calibration is used to construct a matrix in flux and frequency channels for converting observed data into degrees Kelvin. They are then corrected for short time variations by the on-line calibration assuming that the calibration channel is representative for the whole spectrum. The system temperature and, if requested, the background before the event or any other background are subtracted in left, then right circular polarization. Finally, the temperatures are transformed into flux units and degree of polarization, making use of the antenna calibration.

The major sources of error in decreasing importance are (i) poor knowledge of solar flux on the days of antenna calibration and sometimes diverging reports by different observatories, (ii) time variations in ground reflection due to weather or seasonal ground characteristics, and (iii) aging and defects of the feed, cables, and connectors up to the front end. All other variations in the receiver or the front end can be detected from the reference spectra and will normally be corrected automatically during off-line calibration. Errors of the first kind are of the order of 10%. We have followed the spectrum of the quiet Sun over a period of weeks and have found variable deviations in the spectrum of 5% which are probably instrumental, ground reflections, etc. In exceptional cases large narrowband gain reductions of unknown origin have been noted. They can easily be recognized in the spectrum and calibrated out, assuming a flat background.

4. Data Reduction and First Results

The data are analyzed off-line with software that has been developed for the Ikarus spectrometer and considerably expanded over the last years. Figure 2 shows an example of data in spectrogram presentation displayed in two dimensions (flux density in logarithmic scale vs frequency and time). Figure 2(a) is a copy of the film recording by the classic analog spectrograph. Unresolved millisecond spikes are barely visible ≥ 450 MHz, and between 09:33:40 and 09:34:00 UT and 400–600 MHz narrowband type III bursts can be identified. Figure 2(b) shows the spectrogram made from 'Phoenix' data. The time resolution is 0.1 s, and 200 frequency channels were measured. Only few channels were observed below 1 GHz to overlap with the Daedalus range. The frequency resolution and channel width above 1 GHz is 10 MHz. Note the complementary properties of the two spectrometers, in particular the extension of the small group of spikes in the Daedalus range into an enormous cluster in the microwaves. The polarigram of calibrated data is presented in Figure 2(c). The polarization of pixels with flux density below 5 standard deviations above the background is put to 0 (grey).

Figure 3 displays data in selected profiles (cuts through spectrograms) of microwave spikes. In Figure 3(a) time profiles of data are shown that have been gained in a special way: 5 s after 'Phoenix' detected a flare in the 1–2 GHz range it switched to an operating mode in which four single frequencies are sequentially registered at 0.5 ms resolution for about 120 ms each. After 1 min the system goes back into the initial mode, registers some spectra and starts again with single-frequency observations if the flare continues.

Figure 3(b) is a presentation of flux vs frequency. Individual spectra separated by 0.1 s in time are shown. In this set of data the millisecond spikes are not resolved in time, but in frequency (resolution: 10 MHz).

A three-dimensional effect can be introduced into a spectrogram by the presentation of the derivative in one direction (usually from the upper left corner). The positive and negative slopes then produce a 'light and shadow' effect as on geographical maps (cf. Figure 4). The method only works well for structures resolved in time and frequency. For large signal-to-noise ratios it is very sensitive to small flux gradients. It can also be used to enhance the contrast and is well suited to display a multitude of structures. In Figure 4 hundreds of narrowband type III bursts (blips) are visible that occurred during a subflare. The most intense bursts are visible also in second harmonic emission around 2 GHz.

Figure 5 is a fully three-dimensional view of an extremely broadband type III burst (generally accepted to be caused by an electron beam). It extends from 2.8 to 0.3 GHz and is the broadest type III ever observed. A metric type III event is also visible in the first half of the picture. A decimetric type IV develops after 12:39:15 UT. The data have been calibrated, logarithmically compressed, and zoomed. The background just before the microwave-metric type III was subtracted. This display emphasizes spectral evolution but loses most of the time information.

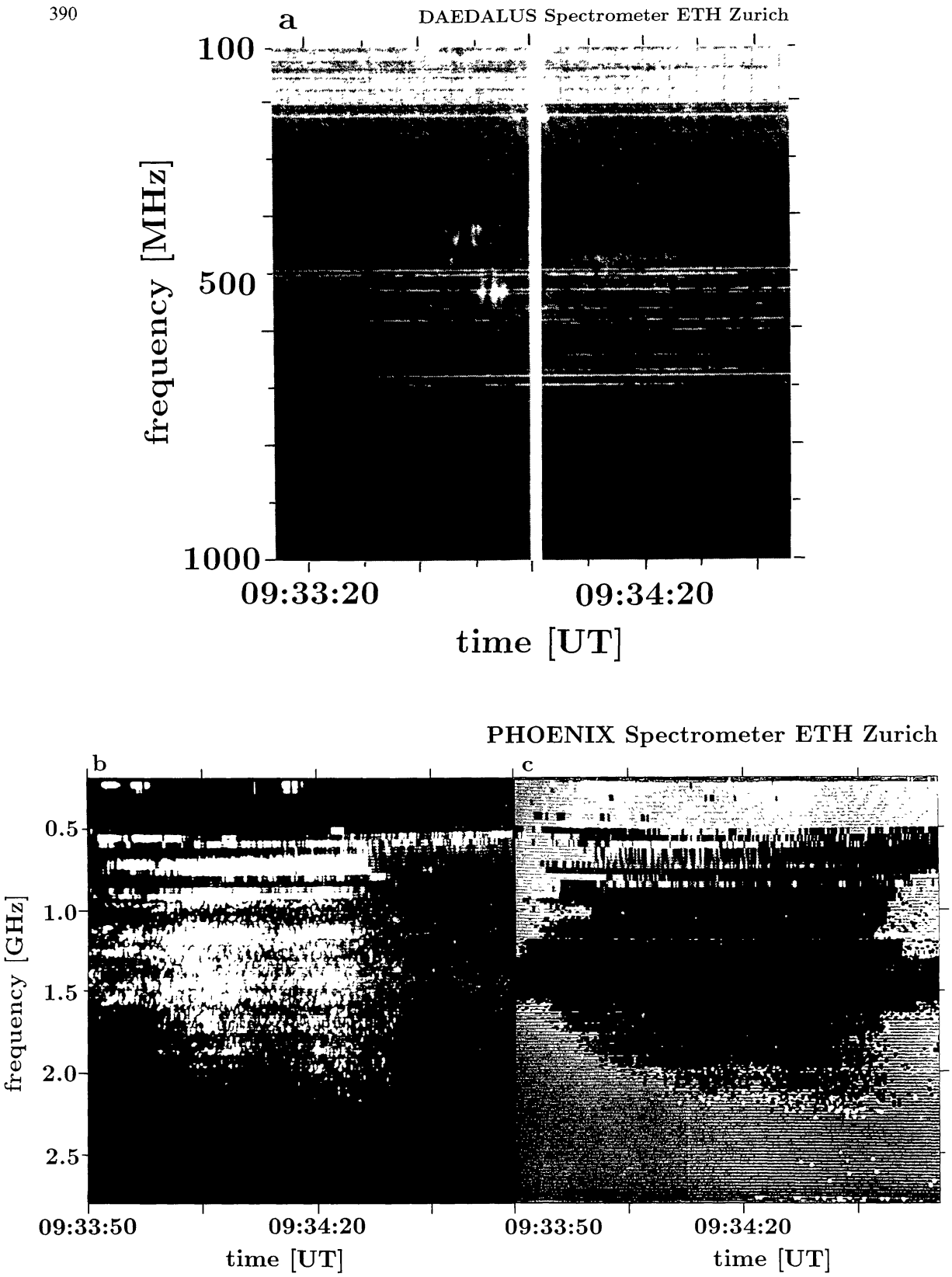

Fig. 2. Spectrogram presentation of type III/spike event of 1989, August 31. (a) Film registration in the metric/decimetric range by 'Daedalus' spectrograph. White is enhanced emission. Terrestrial interference produces horizontal lines. The vertical line is a minute mark. (b) Calibrated data of 'Phoenix' spectrometer concentrating on microwave range. (c) Polarization presented in white (left circular polarization, maximum: 60%) and black (right circular polarization, maximum: 60%). Note left polarized type III bursts and right polarized millisecond spikes.

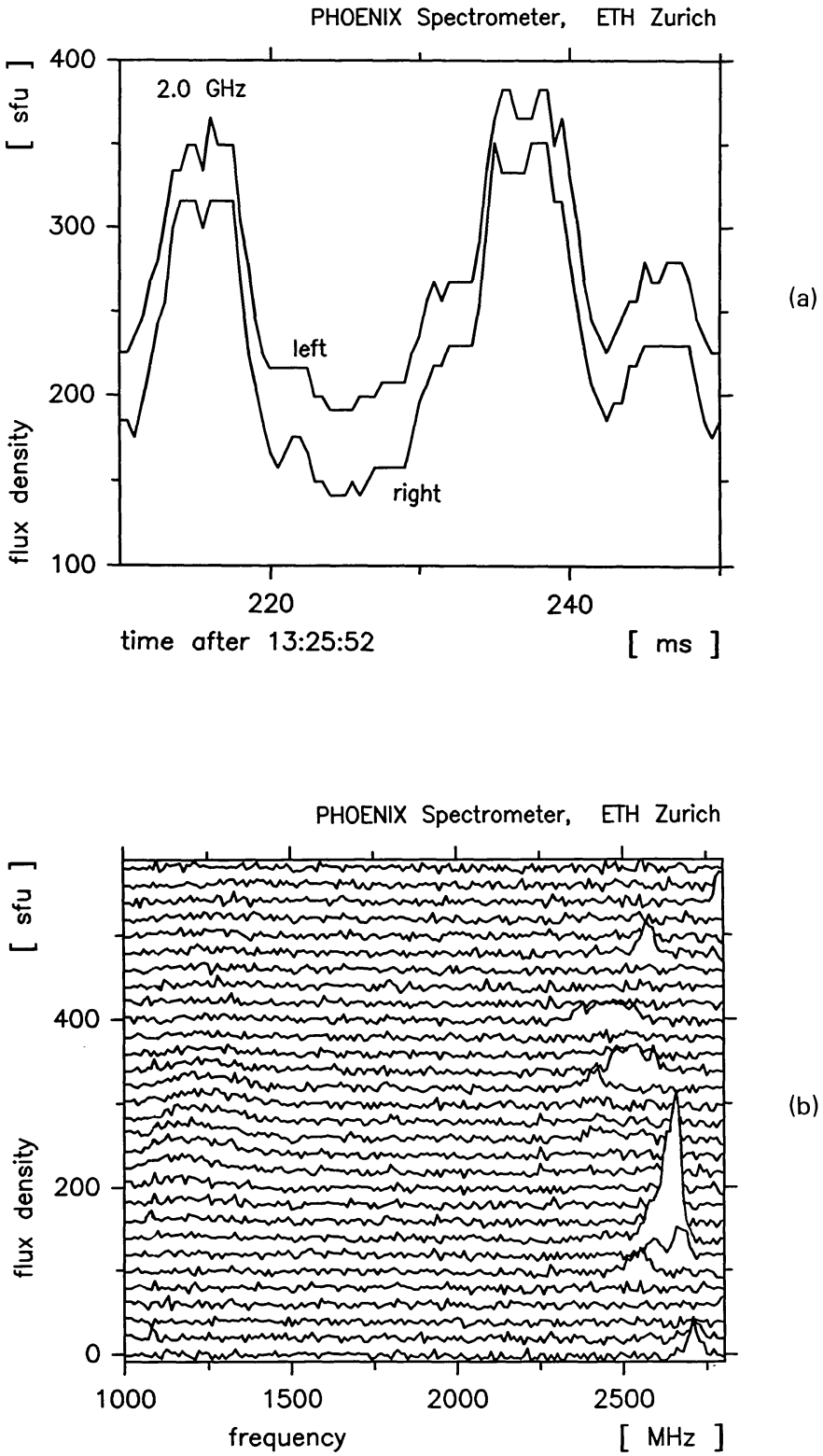

Fig. 3. Presentation of calibrated one-dimensional data by profiles: (a) Time profile at 2.0 GHz of practically unpolarized millisecond spikes observed with 0.5 ms resolution on 1990, January 20. Left circular polarization is shifted by 50 s.f.u. (b) Frequency profiles (spectra) of millisecond spikes observed every 0.1 s on 1989, July 17. The first spectrum at the bottom was taken at 05 : 50 : 44.3 UT. Subsequent spectra are shifted by $n \times 20$ s.f.u. (1 s.f.u. = solar flux unit = 10^{-19} erg cm^{-2} s^{-1} Hz^{-1}). Note also weak continuum 'patch' around 1200 MHz.

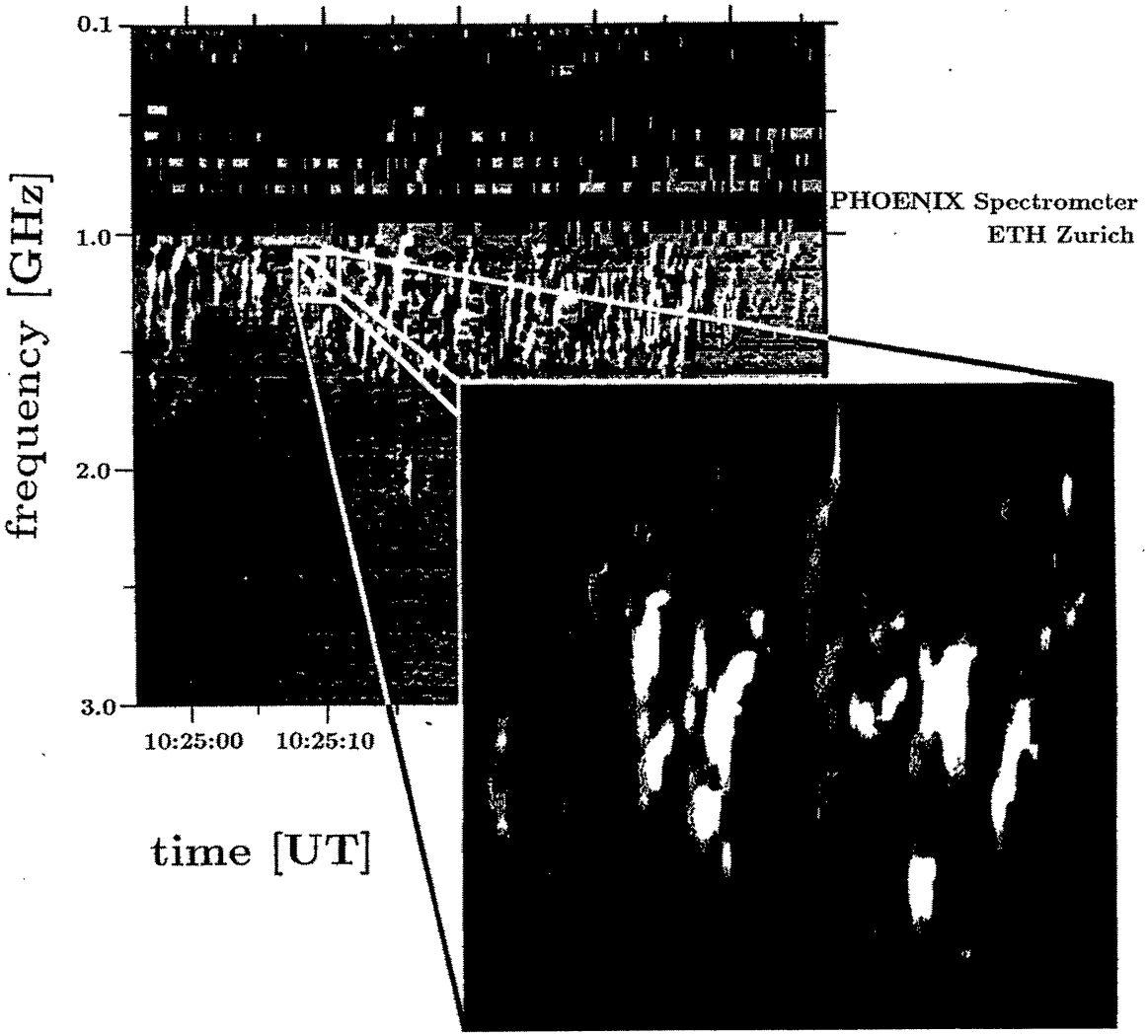

Fig. 4. Pseudo three-dimensional representation of spectrogram by 'light and shadow' effect of a group of narrowband, drifting bursts ('blips', probably type III emission caused by electron beams) observed on 1989, September 26.

5. Conclusions

With the Zürich spectrometer 'Phoenix' now operating in the 0.1–3 GHz band, the gap in the radio spectrum between the well-known decimetric range below 1 GHz and other spectrometers in Bern and Dwingeloo operating at higher frequencies becomes accessible to high-resolution spectrometry. The newly observable band, the low-frequency part of the microwaves, was found to be rich in spectrally structured emission during flares indicative of coherent radiation processes. The free choice of the number, bandwidth, and frequency of the observed channels makes the instrument very flexible for both broadband surveys as well as specific studies at high time or high spectral resolution.

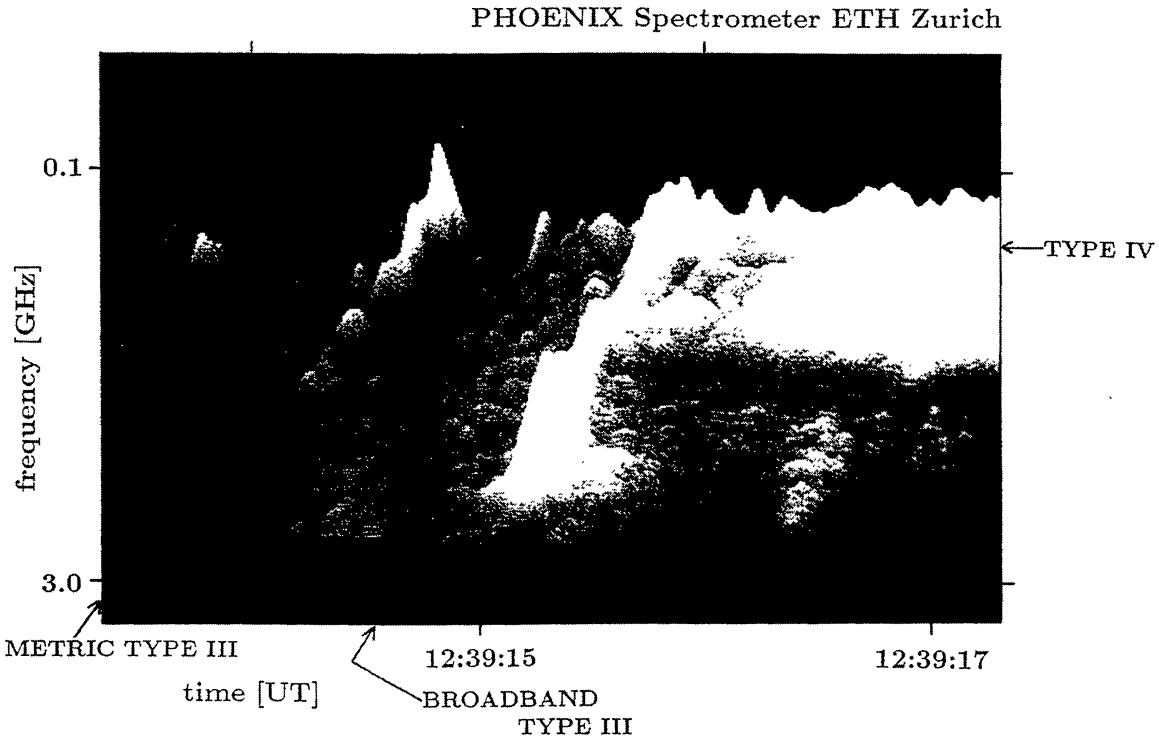

Fig. 5. Three-dimensional representation of spectrogram as flux density (logarithmic, up) vs frequency (left) vs time (forward). The observations were recorded on 1989, September 26. A broadband type III burst traverses the middle of the picture starting at 2.8 GHz.

Acknowledgements

The construction of the Zürich spectrometers is financed by the Swiss National Science Foundation (grant No. 2000–5.499). The design of the 'Phoenix' spectrometer was made by M. R. Perrenoud. Thanks are due to F. Aebersold and A. Wahl for their mechanical work. We also acknowledge contributions by H. Benedickter, T. Maag, D. Meier, P. Povel, and H. Studer.

References

Antonucci, E., Rosner, R., and Tsinganos, K.: 1986, *Astrophys. J.* **301**, 975.
Bruggmann, G., Benz, A. O., Magun, A., and Stehling, W.: 1990, *Astron. Astrophys.* **240**, 506.
Güdel, M. and Benz, A. O.: 1988, *Astron. Astrophys. Suppl. Ser.* **75**, 243.
Perrenoud, M. R.: 1982, *Solar Phys.* **81**, 197.
Tarnstrom, G. L.: 1973, *Astron. Mitt. Eidg. Sternwarte Zürich*, No. 317.
Widing, K. G. and Doyle, J. G.: 1990, *Astrophys. J.* **352**, 760.
Wiehl, H. J., Benz, A. O., and Aschwanden, M. J.: 1985, *Solar Phys.* **95**, 167.
Young, C. W., Spencer, C. L., Moreton, G. E., and Roberts, J. A.: 1961, *Astrophys. J.* **133**, 243.